AIP | Journal of Applied Physics

Semiconducting polymers and quantum dots in luminescent solar concentrators for solar energy harvesting

V. Sholin, J. D. Olson, and S. A. Carter

Citation: Journal of Applied Physics **101**, 123114 (2007); doi: 10.1063/1.2748350
View online: http://dx.doi.org/10.1063/1.2748350
View Table of Contents: http://scitation.aip.org/content/aip/journal/jap/101/12?ver=pdfcov
Published by the AIP Publishing

Articles you may be interested in

Analyzing luminescent solar concentrators with front-facing photovoltaic cells using weighted Monte Carlo ray tracing
J. Appl. Phys. **113**, 214510 (2013); 10.1063/1.4807413

Charge transport in two different conductive polymer and semiconducting quantum dot nanocomposite systems
J. Appl. Phys. **111**, 044313 (2012); 10.1063/1.3682106

Monte-Carlo simulations of light propagation in luminescent solar concentrators based on semiconductor nanoparticles
J. Appl. Phys. **110**, 033108 (2011); 10.1063/1.3619809

Size-tunable infrared (1000–1600 nm) electroluminescence from PbS quantum-dot nanocrystals in a semiconducting polymer
Appl. Phys. Lett. **82**, 2895 (2003); 10.1063/1.1570940

Quantum-dot concentrator and thermodynamic model for the global redshift
Appl. Phys. Lett. **76**, 1197 (2000); 10.1063/1.125981

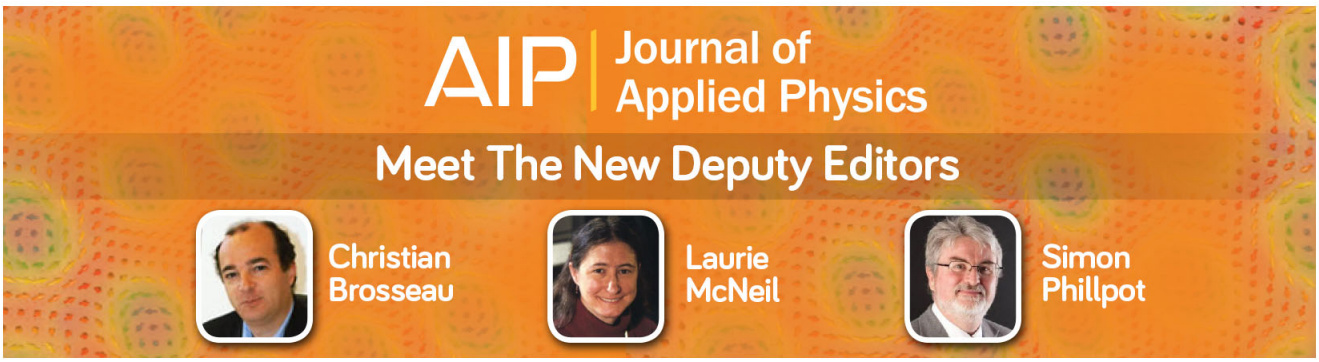

[This article is copyrighted as indicated in the article. Reuse of AIP content is subject to the terms at: http://scitation.aip.org/termsconditions. Downloaded to] IP: 128.114.130.190 On: Fri, 30 Jan 2015 22:00:09

Semiconducting polymers and quantum dots in luminescent solar concentrators for solar energy harvesting

V. Sholin, J. D. Olson, and S. A. Carter[a)]
Physics Department, University of California—Santa Cruz, Santa Cruz, California 95064

(Received 31 January 2007; accepted 2 May 2005; published online 28 June 2007)

We compare the performance of luminescent solar concentrators (LSCs) fabricated with polymers and quantum dots to the behavior of laser dye LSCs. Previous research, centered around the use of small molecule laser dyes, was hindered by the lack of materials with small absorption/emission band overlap and longer lifetime. Materials such as semiconducting polymers and quantum dots present qualities that are desirable in LSCs, for example, smaller absorption/emission band overlap, tunable absorption, and longer lifetimes. In this study, the efficiency of LSCs consisting of liquid solutions of semiconducting polymers encased in glass was measured and compared to the efficiency of LSCs based on small molecule dyes and on quantum dots. Factors affecting the optical efficiency of the system such as the luminescing properties of the organic materials were examined. The experimental results were compared to Monte Carlo simulations. Our results suggest that commercially available quantum dots cannot serve as viable LSC dyes because of their large absorption/emission band overlaps and relatively low quantum yields. Materials such as Red F demonstrate that semiconducting polymers with high quantum yield and small absorption/emission band overlap are good candidates for LSCs. © *2007 American Institute of Physics*.
[DOI: 10.1063/1.2748350]

INTRODUCTION

Recent developments in visible and infrared-emitting semiconducting polymers and quantum dots have opened up opportunities for higher efficiency luminescent solar concentrators (LSCs). LSCs are waveguides consisting of a slab of highly transparent material doped with a fluorescent dye. Photons incident on the slab are down-converted by the fluorescent molecules, waveguided toward the edges of the structure, and then photovoltaically converted by detectors coupled to the edges of the LSC. LSCs have several advantages over traditional optical solar concentrators. LSCs will accept both direct and diffuse light, so that a precise solar tracking method is not an essential component of the system. It has been shown,[1,2] in fact, that LSCs have better performance under diffuse light than under direct light. In addition to this, the extended surface area of LSCs allows heat lost by solar photons to be dispersed. In this way the detector coupled at the edges will receive "cool" photons and thus will work more efficiently. Furthermore, the dye is chosen so that its absorption band overlaps with the peak emission of the sun and its emission occurs at a wavelength range at which the detector is efficient. Finally, LSCs have the advantages of architectural integrability and lower cost.

The efficiency of the LSC depends on the spectral properties of the dye and the matrix, as well as the geometric properties of the structure. It is required that the dye absorb efficiently a broad portion of the solar spectrum, that it emit efficiently (high quantum yield), and that there be small absorption/emission band overlap, often quantified by measuring the Stokes shift. This last requirement is necessary in order to avoid reabsorption of photons once these have been emitted by the fluorescing molecules. Finally, the structure must maximize the amount of trapping at the top and bottom surfaces and minimize the amount of trapping at the collection edges. This will be determined by the shape of the structure as well as by the index of refraction of the matrix. Shurcliff and Jones[3] calculated the amount of light trapped in such a structure: about 75%, assuming the index of refraction of the LSC is 1.5.

LSCs were proposed by Weber and Lambe[4] and studied most intensely during the 1980s.[5–14] Most of this research involved the use of laser dyes as the fluorescent species in the LSC. Rhodamines, coumarins, and 4-dicyanomethylene-2-methyl-6-(p(dimethylamino)styryl)-4H-pyran (DCM) were common choices because these materials have extremely high quantum yields and they are inexpensive compared to inorganic fluorescent dyes. Relatively large self-absorption of the dyes' emission and short dye lifetimes negatively dominated the behavior of the LSCs,[5,8,15] however, hindering the advancement of this research. Nevertheless, various aspects of LSC performance are currently being studied.[2,16,17]

The synthesis of materials such as semiconducting polymers and quantum dots provides an opportunity to improve the performance of the LSCs. Polymers synthesized for the organic light-emitting diode industry often have extremely high quantum yields, and polymer lifetimes have been reported to be longer than that of small molecules.[18] Semiconducting polymers have not been applied to LSCs as of the publication of this work. Quantum dots with passivated surfaces may also present high quantum yields and longer lifetimes.[19] In addition to this, it is possible to synthesize quantum dots in sizes such that their absorption and emission curves lie appropriately in relation to the sun's emission

[a)]Electronic mail: sacarter@ucsc.edu

 © 2007 American Institute of Physics

[This article is copyrighted as indicated in the article. Reuse of AIP content is subject to the terms at: http://scitation.aip.org/termsconditions. Downloaded to] IP: 128.114.130.190 On: Fri, 30 Jan 2015 22:00:09

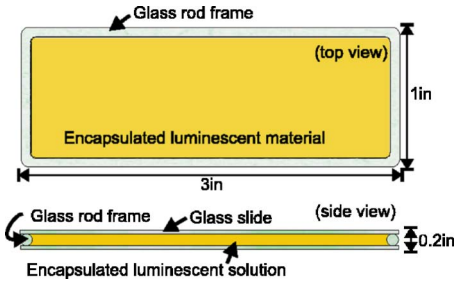

FIG. 1. (Color online) Top and side views of the structure of the LSCs in this study. A glass frame is sandwiched between two microscope slides to form an enclosure that holds the luminescent solution.

spectrum and the detection range of the detector. Some studies have already explored the use of quantum dots in LSCs.[17,20]

EXPERIMENT

Since organic materials degrade in the presence of oxygen excited by light, various approaches have been taken to protect the active materials from contact with oxygen. Avnir *et al.*[21] and Reisfeld *et al.*[22] embedded rhodamine and perylimide dyes in a sol-gel matrix to isolate the fluorescing molecules from each other and from their surroundings. Mansour *et al.*[2,23] copolymerized coumarin 6 and perylene with styrene and methyl methacrylate to obtain more stable LSCs. Our approach has been to encapsulate the fluorescent dyes in glass boxes. Glass was chosen because, among the materials that will efficiently hinder oxygen diffusion, it is the densest and the least expensive. A glass rod was bent into a rectangular frame and then glued between two microscope slides. A schematic of the cell structure is shown in Fig. 1. The size of the LSCs was approximately $1\times3\times0.2$ in.^{3}. The geometric gain G is defined by $G=A_{\text{top}}/A_{\text{edge}}$, where A_{top} is the area of the LSC illuminated by the light source, and A_{edge} is the area of the collecting edge; G has a value of around 16 for our experimental samples. Batchelder *et al.*[15] have shown that optical efficiency decreases with increase in geometric gain. Their results indicate that a geometric gain on the order of 10, such as that of our samples, represents a good balance between high geometric gain and high optical efficiency.

Liquid solutions of the fluorescing materials were introduced into the glass enclosure through a small opening in the frame, which was then sealed. Depending on the solvent of the dye, either a simple transparent two-part epoxy or a UV-curable Addison Clear Wave epoxy was used to fabricate the enclosure. For the latter case, care was taken to protect the dye as the seal was cured with UV light. The initially clear UV-curable epoxy became orange upon curing, but this discoloration did not seem to affect the performance of the LSCs significantly. We chose to work with liquid solutions since liquids would most easily mold to the glass enclosure we wished to provide. Additionally, in a practical setting liquid solutions have the advantage of easy dye replacement upon dye degradation. Nevertheless, the use of liquid solutions limits the index of refraction of the matrix, and from this perspective, the use solid matrices is preferable. Since the fluorophores used in this work are dissolved in the same

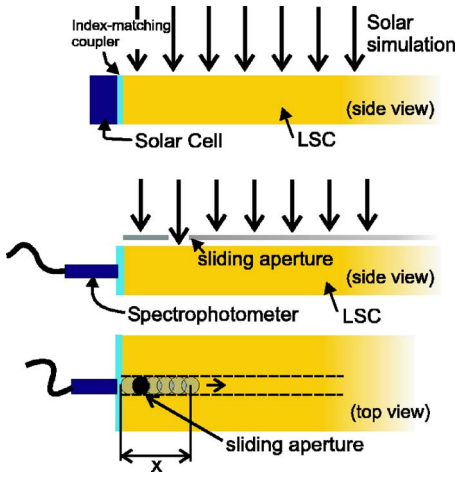

FIG. 2. (Color online) Experimental setup. The LSC can be coupled to a solar cell or a spectrophotometer. The top of the LSC can be fully illuminated or partially illuminated by use of a mask containing an aperture that can slide along the length of the LSC.

solvents that dissolve materials such as polymethyl methacrylate (PMMA) or polystyrene, embedding them in a highly transparent, high index of refraction solid matrix should be straightforward. In addition to this, semiconducting polymers themselves have high indices of refraction, and in this sense, they will complement the high index of the matrix.

Rhodamine B (Exciton), a high quantum yield laser dye, was chosen to construct control devices. The need for materials with small absorption/emission band overlap prompted us to test two additional laser dyes: LDS698 and LDS821 (Exciton). The semiconducting polymers MDMO-PPV (Aldrich), MEH-DOO-PPV, and a red polyfluorene (Red F) were tested. CdHgTe (ADS820QD from ADS Dyes) and CdSe/ZnS core-shell quantum dots (Evident Technologies) were tested as well; however, CdHgTe presented quantum yields too low for successful application in LSCs.

Solutions of all dyes except the quantum dots were made by preparing stock solutions of each dye and stirring these for 24 h on a hotplate. The laser dyes were dissolved in a propylene carbonate and ethylene glycol mixture in a 15:85 ratio by volume. The polymers were dissolved in chlorobenzene. The CdSe/ZnS quantum dots were provided dispersed in toluene by the vendor. Lower concentrations of each dye were obtained by dilution of the respective stock solutions. This procedure was followed for concentration dependence studies as well as for fabrication of the LSCs.

Steady-state absorption spectra were taken with an n&k UV-vis spectrometer. Steady-state photoluminescence (PL) spectra were measured with an LS-45 Perkin Elmer spectrometer. Radiance and current attenuation curves with increase in source-detector distance were measured with the aid of a specifically designed tester. The testing mount was built to hold the LSC under the light source and against a silicon solar cell or spectrophotometer (Fig. 2). In the tester, the LSC lies in a trough and it was coupled to either a commercially available single-crystalline solar cell (Silicon Solar, measured power efficiency of 3%) or to an Ocean Optics charge-coupled device (CCD) array spectrophotometer.

[This article is copyrighted as indicated in the article. Reuse of AIP content is subject to the terms at: http://scitation.aip.org/termsconditions. Downloaded to] IP: 128.114.130.190 On: Fri, 30 Jan 2015 22:00:09

When appropriate, partial illumination of the top surface of the LSC was achieved by use of a mask containing a 0.5 cm diameter aperture on a rail. As shown in Fig. 2, the aperture could slide along the length of the cell, allowing for measurements of light intensity or current as a function of detector/source distance. The tester was matte black, thus avoiding reflection of escaped photons back into the LSC. The light source for measurement of the redshift due to reabsorption was a white light-emiting diode (LED) in order to achieve higher emission signals; a solar simulator was used for measurement of optical efficiency. The LSC was coupled to the detector with Saint-Gobain optical grease.

Estimates of the quantum yield (QY) of the dyes used in this work were measured in the laboratory. This was accomplished by measuring the fluorescence intensity of the dye solutions relative to that of rhodamine B, which is known to have a quantum yield of around 0.95 in ethanol.[24,25] Solutions were prepared at concentrations such that the optical density (OD) was equal to 0.05 at the wavelength of peak emission of the light source to minimize self-absorption effects. The optical density is defined as $OD=\alpha Cd$, where α $(M\ cm)^{-1}$ is the absorption coefficient of the dye, C (M) is the concentration, and d (cm) is the thickness of the sample. The light source was a Luxeon blue LED emitting around 200 cd on axis. The detector was a calibrated CCD array Ocean Optics spectrophotometer. A 1 cm path length cuvette in a right-angle geometrical arrangement was used to measure the fluorescence spectra. To calculate the quantum yield of the dyes, the area of the emission of rhodamine B was normalized to 0.95, and the integrated emission spectra of the rest of the dyes were scaled accordingly.

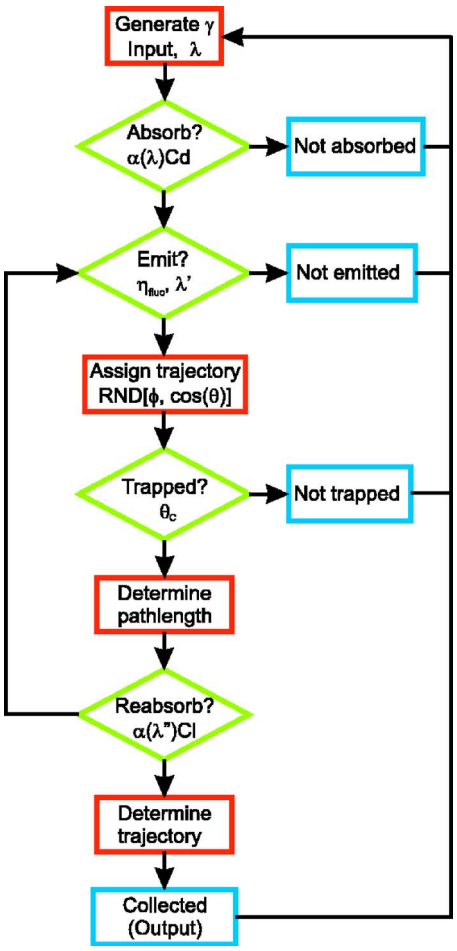

FIG. 3. (Color online) Schematic representation of the Monte Carlo simulations program.

MONTE CARLO SIMULATIONS

Monte Carlo simulations of the behavior of the LSCs were performed. A flowchart representation of the simulations is shown in Fig. 3. The program relies on the quantum yield, the wavelength-dependent absorption coefficient, and the emission spectrum of the dye, all of which were obtained experimentally, as well as on the spectrum of the sun's emission, obtained from NREL. The simulation begins by assigning a wavelength λ to an incoming photon according to the solar spectrum. Based on the absorption coefficient of the dye, the concentration of the dye, and the cell thickness, the program then calculates a probability of absorption. To determine if the dye will fluoresce, the simulation checks a random number against the material's quantum yield; a random number higher than the material's quantum yield results in a photon that is lost to mechanisms competing with fluorescence, whereas a random number lower than the material's quantum yield results in an emitted photon. In the latter case, the program chooses an emission wavelength λ′ according to the emission spectrum of the dye.

A random direction is assigned to the photon, and the program determines if the photon is trapped by means of total internal reflection. Based on the absorption coefficient of the dye, a random number determines the distance the photon will travel. At this point, the program decides whether or not the photon will intersect a collecting edge before being reabsorbed. In the case the photon will not intersect a collecting edge, it gets reabsorbed and is given another chance to be emitted according to the criteria given above. In the case the photon will intersect a collecting edge, then the simulation locates the photon close to the collecting edge and determines its path. It chooses a random height for the photon and then determines the reflections and refractions according to the photon's angle of incidence with respect to the interfaces and its polarity as well as the relative indices of the media on either side of the interfaces. Once the photon has been collected at an edge or lost, the program begins again with a different photon. The program inputs a total of 100 000 photons and does not account for variations in the quantum yield with concentration.

RESULTS

We sought materials with broad absorption bands, high quantum yields, and large Stokes shifts. Table I shows several spectroscopic properties of the dyes tested as measured in our laboratories. The laser dyes LDS698 and LDS821, as well as the polymer Red F and the CdSe/ZnS core-shell quantum dots, present Stokes shifts of over 200 nm. Figure 4 shows the normalized absorbance and radiance spectra for CdSe/ZnS and LDS821. Also shown are the emission spectrum of the sun (AM1.5 Direct) and the responsivity of sili-

[This article is copyrighted as indicated in the article. Reuse of AIP content is subject to the terms at: http://scitation.aip.org/termsconditions. Downloaded to] IP: 128.114.130.190 On: Fri, 30 Jan 2015 22:00:09

TABLE I. Spectroscopic properties of the dyes used in this work as measured in our laboratories. QY is the quantum yield of the dye, α_{max} is the maximum value of the absorption coefficient, $\lambda(\alpha_{max})$ is the expectation value of the absorption coefficient, $\lambda(PL_{max})$ is the expectation value of the emission, $\Delta\lambda_{Stokes}$ is the Stokes shift of the dye, η_{St} is the Stokes efficiency defined as $\lambda(\alpha_{max})/\lambda(PL_{max})$, and the last column represents the redshift in the emission spectra as the light source travels 6 cm down the LSC.

Material	QY	α_{max} $(M\ cm)^{-1}$	$\lambda(\alpha_{max})$ (nm)	$\lambda(PL_{max})$ (nm)	$\Delta\lambda_{Stokes}$ (nm)	η_{St}	Redshift (nm)
Rhodamine B	0.95	1.5×10^5	550	629	79	0.87	23
LDS698	0.11	6.9×10^4	466	685	219	0.68	11
LDS821	0.09	7.7×10^4	557	802	246	0.69	13
MDMO-PPV	0.45	2.8×10^4	460	592	132	0.78	31
MEH-DOO-PPV	0.48	6.9×10^4	467	593	127	0.79	34
Red F	0.67	1.8×10^7	413	657	244	0.63	13
CdSe/ZnS	0.50[a]	3.6×10^6	376	623	248	0.60	32

[a]Value provided by vendor.

con, which peaks at 1000 nm. Silicon is the material we use as a detector. The figure emphasizes that while both materials have large Stokes shifts, the absorption/emission band overlap is small for LDS821 but large for CdSe/ZnS. Owing to the strong absorption in the UV, the expectation value of the absorption of CdSe/ZnS lies in the blue part of the spectrum, which results in a large Stokes shift. The overlap of the two bands is large, however, because the emission is narrow. Even if the Stokes shift and the size of the overlap correlate well for the rest of the materials used, the data for CdSe/ZnS show that the Stokes shift alone is not necessarily a good quantifier for the absorption/emission band overlap and thus the amount of self-absorption occurring in the LSC. Additionally, the data evidence that this characteristic of quantum dots must be addressed in order for this type of material to be used in an efficient LSC.

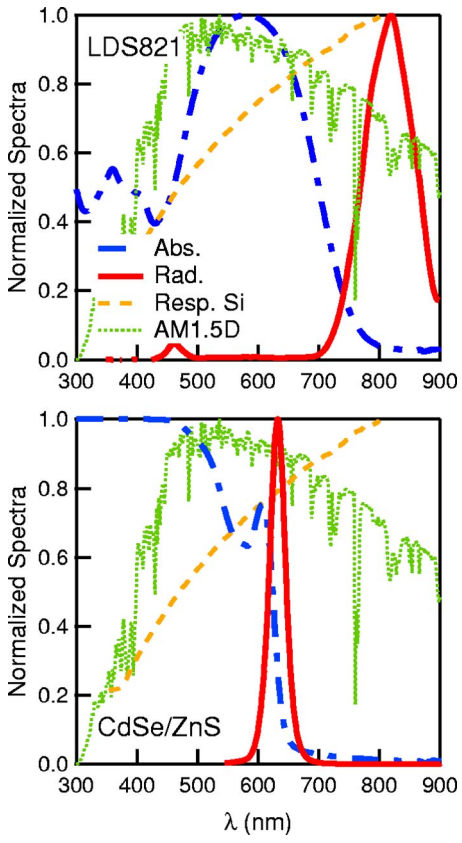

FIG. 4. (Color online) Normalized absorbance and radiance spectra for the laser dye LDS821 and CdSe/ZnS quantum dots in relation to the emission spectrum of the sun (AM1.5 Direct) and the responsivity of silicon. The responsivity of silicon peaks at 1000 nm.

While a high dye concentration in LSCs will ensure plentiful absorption of solar photons, it will also lower the quantum yield because of the formation of quenching dye aggregates. As a result of this, the concentration of the dye must be chosen in order to balance these two effects in favor of maximizing the efficiency of the device. With this purpose, we measured the dependence of absorption and steady-state PL of each dye on concentration using a 1 cm path length cuvette. The absorption efficiency η_{abs} was calculated for each sample according to the equation[4]

$$\eta_{abs} = \frac{\int^{\lambda_c} N(1-T)d\lambda}{\int^{\lambda_c} Nd\lambda},$$

where N is the solar photon flux, T is the transmittance of the dye, and λ_c is the cutoff wavelength of the detector (silicon in this work). The transmittance T is measured directly by our n&k UV-vis spectrometer and is defined as $T=\exp(-\alpha Cd)$.

Figure 5 compares the dependence of the PL peak intensity and absorption efficiency on concentration for the polymer Red F and the CdSe/ZnS quantum dots. The concentration for peak emission, occurring around $6\times10^{-8}M$ for Red F and around $1.5\times10^{-6}M$ for the quantum dots, does not coincide respectively with the concentration for maximum absorption, occurring around $8\times10^{-6}M$ for Red F and around $3\times10^{-6}M$ for the quantum dots. The upper limit of concentration for the materials used in this work was set by the limit of solubility of the material in the case of the laser dyes and the polymers, or by the concentration of the original solution received from the vendor in the case of quantum dots. Therefore, even though the absorption efficiency curve has not completely saturated as concentration increases in the plots presented, we do not consider that higher absorption efficiencies were experimentally possible. We note that a

[This article is copyrighted as indicated in the article. Reuse of AIP content is subject to the terms at: http://scitation.aip.org/termsconditions. Downloaded to] IP: 128.114.130.190 On: Fri, 30 Jan 2015 22:00:09

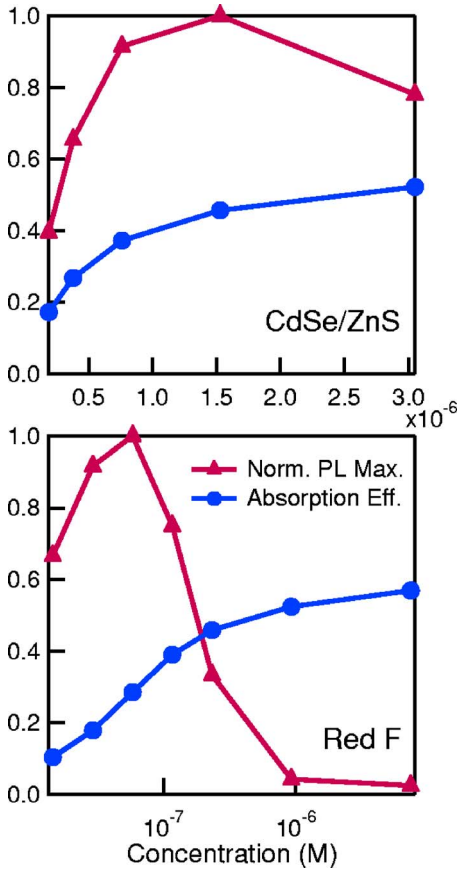

FIG. 5. (Color online) Concentration dependence of the PL maximum (normalized) and the absorption efficiency of the CdSe/ZnS core-shell quantum dots and the polymer Red F.

high concentration will not only reduce the quantum yield of the dye but will also promote self-absorption by shortening the path length of the photons. It is therefore desirable to find the optimum concentration that will balance out these phenomena. LSCs of dye concentrations that maximized absorption efficiency or maximized PL, as well as LSCs of intermediate dye concentrations, were fabricated.

Figure 6 shows the dependence of optical efficiency on concentration for the laser dye LDS821 and the polymer MDMO-PPV. While the definition of optical efficiency and the conditions for its measurement will be described below, it is important to note at this stage that the concentration for highest efficiency LSC for each material is closer to the concentration for highest absorption efficiency than to the concentration for highest emission. The results suggest that concentration should be raised at the expense of quantum yield (emission) in order to favor absorption. This result has been previously calculated by Batchelder *et al.*[7]

Because photons must usually travel large distances before reaching the collection edge, overlap of the absorption and emission bands is a serious impediment for high efficiency LSCs. By partially illuminating the surface of the LSC through an aperture that slides along the length of the LSC and thus increasing the source/detector distance (see Fig. 2), the path length of the emitted photons increases. This increases the probability of reabsorption. Figure 7 shows the redshift in emission spectra for the polymer Red F, the

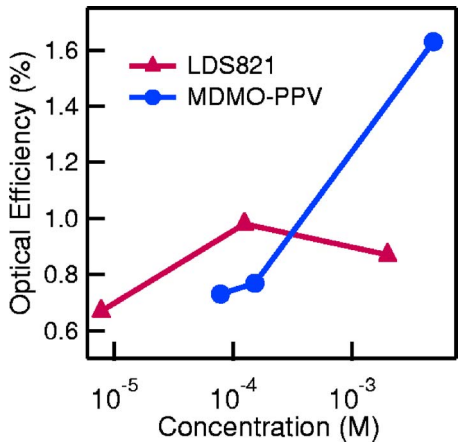

FIG. 6. (Color online) Optical efficiency as a function of concentration for the laser dye LDS821 and the polymer MDMO-PPV.

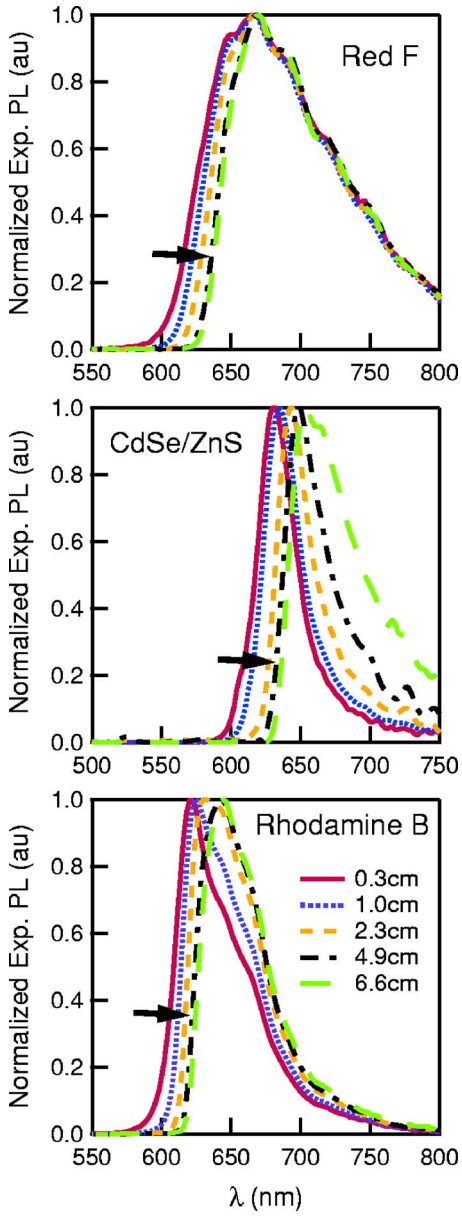

FIG. 7. (Color online) Experimental redshift of the emission spectra for the polymer Red F, the CdSe/ZnS quantum dots, and the laser dye rhodamine B as the light source slides along the length of the LSCs. The emission spectra have been normalized.

[This article is copyrighted as indicated in the article. Reuse of AIP content is subject to the terms at: http://scitation.aip.org/termsconditions. Downloaded to] IP: 128.114.130.190 On: Fri, 30 Jan 2015 22:00:09

CdSe/ZnS quantum dots, and the laser dye rhodamine B. The decay in the blue tail of the emission spectra evidences that reabsorption of emitted photons increases with increasing path length. The amount of redshift is reported in Table I. Of the materials presented, Red F has the smallest redshift in the emission. Because polymers undergo a change in structural conformation when excited, the Stokes shifts are usually large and this may be accompanied by small absorption/emission band overlaps, which leads to smaller redshifts. Quantum dots do not undergo structural changes when excited, and this leads to large absorption/emission band overlaps and large redshifts.

One way of reducing the amount of redshift is to control the amount of absorption/emission band overlap during synthesis of the materials. The general profile of the bands and the general position of the peak of the bands are determined by the electronic structure of the materials. The width of the bands, however, is also related to the distribution of polymer chain lengths in the case of polymers and to the distribution of dot sizes in the case of quantum dots:[26] the larger the distribution of chain lengths or dot sizes, the wider the bands. Hence, a large distribution of chain lengths (or dot sizes) leads to larger absorption/emission band overlap and larger redshifts. Therefore, control over the distribution of chain lengths in polymer samples and of dot sizes in quantum dot samples would lead to smaller redshifts and thus to improved LSC performance.

Figure 8 shows the experimental and simulated expectation values of the emission spectra as a function of source/detector distance for several concentrations of Red F, CdSe/ZnS, and rhodamine B. We report the expectation value of the spectra rather than the wavelength of the peak in order to account for the changes in the spectra that occur as a consequence of reabsorption. For each concentration, the emission redshifts as the source/detector distance increases, reflecting the results shown in Fig. 7. An overall concentration-dependent redshift is also visible for each material: the expectation value curve for a higher concentration sample is redshifted with respect to a lower concentration one. This is expected as higher concentration samples have shorter absorption lengths, and therefore, photons emitted in these samples are more prone to reabsorption. Most reabsorption will occur within a few centimeters from the edge of the LSC, as suggested by the saturation in the curves shown in Fig. 8.

In this study we focus on experimentally measuring the integrated optical efficiency η_{opt} of the LSC. The optical efficiency is given by

$$\eta_{opt} = \frac{I_{edge} A_{top}}{I_{det} A_{edge}},$$

where I_{edge} is the short-circuit current of the solar cell coupled to the LSC when the LSC is illuminated from the top, I_{det} is the short-circuit current measured by the solar cell under direct illumination by the light source, and A_{top} and A_{edge} are as defined previously. This equation does not account for the dependence of silicon's responsivity on wavelength or imperfections in the LSC/solar cell coupling. Most of our dyes emit in a similar wavelength range, however, allowing us to assume that the silicon solar cell is converting photons into current similarly for all of our dyes. For measurement of I_{edge}, the three remaining noncollecting edges of the LSCs were painted black in order to simulate collection at those edges and thus avoid collection of photons reflected back into the cell from noncollecting edges.

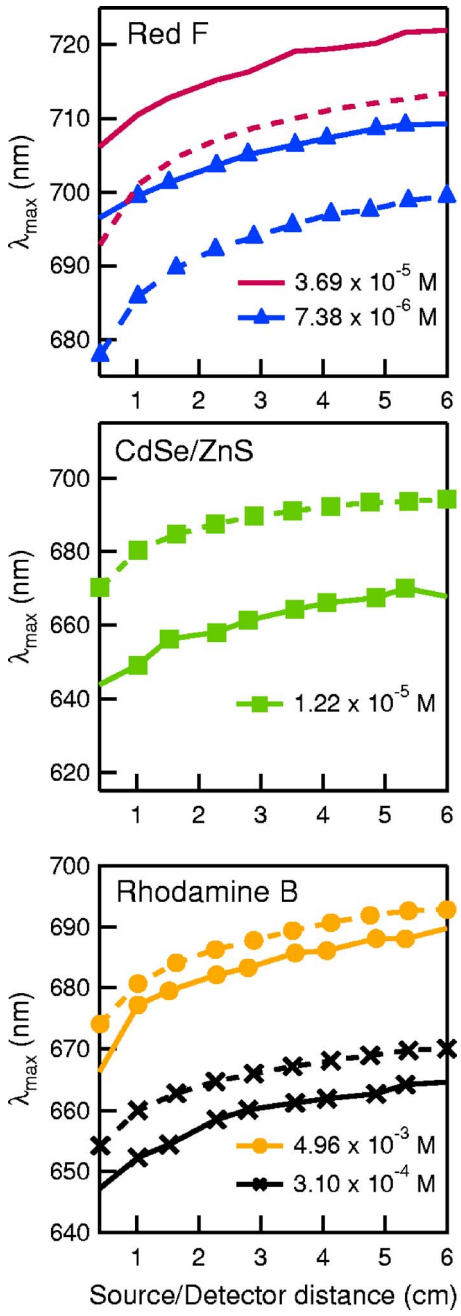

FIG. 8. (Color online) Experimental (solid lines) and simulated (dotted lines) expectation value of the emission for LSCs of Red F, CdSe/ZnS, and rhodamine B.

The experimental setup allows us to find the optical efficiency for single-edge collection, where collection occurs along a 1 in. side of the LSC (see Figs. 1 and 2). Monte Carlo simulations allow the calculation of optical efficiency arising from single-edge or full-perimeter collection. Therefore the simulations yield the geometric factor that relates single-edge collection to full-perimeter collection. Simulated

[This article is copyrighted as indicated in the article. Reuse of AIP content is subject to the terms at: http://scitation.aip.org/termsconditions. Downloaded to] IP: 128.114.130.190 On: Fri, 30 Jan 2015 22:00:09

TABLE II. Simulated optical efficiency of LSCs for single-edge and full-perimeter collection. For single-edge measurements, collection was obtained along a 1 in. side of the LSC.

Material	η_{opt}, single edge (%)	η_{opt}, full perimeter (%)
Rhodamine B	3.9	22.5
LDS698	0.7	3.6
LDS821	0.5	3.4
MDMO-PPV	1.7	9.3
MEH-DOO-PPV	1.9	10.9
Red F	3.8	21.4
CdSe/ZnS	0.4	2.3

TABLE III. Experimental single-edge collection optical efficiency (left) and predicted experimental full-perimeter collection optical efficiency (right) for the LSCs listed in Table II. The values for full-edge collection are obtained by use of the geometric factor calculated from simulations data (Table II).

Material	η_{opt}, expt., single edge (%)	η_{opt}, predicted, full perimeter (%)
Rhodamine B	2.6	15.3
LDS698	0.6	3.6
LDS821	0.5	2.9
MDMO-PPV	1.0	5.9
MEH-DOO-PPV	0.9	5.0
Red F	3.4	19.8
CdSe/ZnS	0.3	1.6

optical efficiencies for the most efficient LSCs of each of the dyes tested in this work are shown in Table II. From these data, we can extract an average geometric factor of 5.8 that relates single-edge collection to full-perimeter collection.

Table III shows the experimental single-edge collection optical efficiency for the same cells presented in Table II. Multiplying these values by the geometric factor obtained through simulations yields an estimate for the experimental full-perimeter collection optical efficiency. The experimental values are consistently less than or equal to the corresponding theoretical values. This discrepancy is attributed mainly to transport losses in the LSC and the decrease of quantum yield with concentration, neither of which are taken into account in the simulations. Nevertheless, dependence of silicon's responsivity on the wavelength and variations in the LSC/detector coupling also contribute to the discrepancy in the results.

The values reported in Table III correspond to the highest efficiency LSC obtained for each material. As mentioned earlier, the concentration of each of the materials was close to the concentration for maximum absorption efficiency. These data show that among the materials tested the polymer Red F is the most suitable dye for use in LSCs, and its performance compares favorably with rhodamine B. This is due to its good absorption/emission band separation, as evidenced by the small redshift relative to that of other dyes (Table I and its relatively high quantum yield. In addition to this, its absorption band and emission band are both broad. We believe that the poorer performance of the polymers MDMO-PPV and MEH-DOO-PPV can be attributed to their low quantum yields, although these materials also display larger absorption/emission band overlap than Red F. The laser dyes LDS698 and LDS821 both present small absorption/emission band overlap, but unfortunately their quantum yields are too low to make successful LSCs. Finally, CdSe/ZnS shows an extremely low optical efficiency. Apart from low quantum yield, the quantum dots suffer from large self-absorption, as will be argued below.

Counters in the simulations allow one to keep track of the final destination of photons. Data of this type are presented in Table IV. Each photon input into the simulation is counted in one of the following categories: photons that were not absorbed as they initially traversed the LSC, photons that were collected (the optical efficiency), photons that were reabsorbed and remitted but not trapped through total internal reflection, and finally, photons that were absorbed but never remitted due to losses to other forms of energy. In the last column, we have added the percentage of photons absorbed but not trapped to those that are simply never remitted. This represents a combination of the effects of quantum yield and self-absorption. The table shows that the number of photons absorbed is essentially the same for the LSCs shown; however, the number of photons lost to poor emission of the dye and large absorption/emission band overlap is 65% larger for the quantum dots than for the polymer. To produce the last row of the table, we have run the simulation assuming that the CdSe/ZnS particles have the same quantum yield as the polymer Red F. This now allows us to directly compare the effects of absorption/emission band overlap for the two ma-

TABLE IV. Breakdown of the final destination of the photons obtained through simulations for the Red F (top row) and CdSe/ZnS (central row) LSCs presented in the previous tables. The last row is produced by assuming the same quantum yield for CdSe/ZnS as for Red F. "Not absorbed" refers to the solar photons that were not absorbed as they traversed the LSC, "Collected" refers to the optical efficiency of the LSC, "Reabsorbed, not trapped" indicates the percentage of photons that were reabsorbed and remitted but not trapped through total internal reflection, and "Not emitted" refers to the percentage of photons that were absorbed but never emitted due to quantum yield of the dye. The last column, "Absorbed, but lost" is the sum of the columns "Reabsorbed, not trapped" and "Not emitted."

Material	QY assumed	Not absorbed	Collected	Reabsorbed, not trapped	Not emitted	Absorbed, but lost
Red F	0.70	46.2	21.4	9.8	22.3	32.1
CdSe/ZnS	0.50	44.8	2.2	9.1	43.9	53.0
CdSe/ZnS	0.70	44.2	5.19	17.1	33.4	50.5

[This article is copyrighted as indicated in the article. Reuse of AIP content is subject to the terms at: http://scitation.aip.org/termsconditions. Downloaded to] IP: 128.114.130.190 On: Fri, 30 Jan 2015 22:00:09

TABLE V. Comparison of the simulated full-perimeter collection optical efficiency for rhodamine B, Red F, and CdSe/ZnS. The last two rows represent the results of the simulation for Red F and CdSe/ZnS assuming the same quantum yield as that of rhodamine B (0.95).

Material	QY assumed	η_{opt}, full perimeter (%)
Rhodamine B	0.95	22.5
Red F	0.70	21.4
CdSe/ZnS	0.50	2.3
Red F	0.95	33.9
CdSe/ZnS	0.95	13.6

terials by comparing the values in the last column. The 18.4% difference in percentages absorbed but lost can be directly attributed to 18.4% more self-absorption occurring in CdSe/ZnS than in Red F. This result shows that the absorption/emission band overlap in commercially available quantum dots is a limiting factor to their use in efficient LSCs.

Table V compares the full-perimeter collection optical efficiency for rhodamine B, Red F, and CdSe/ZnS obtained through simulations. The last two rows present the results obtained from the simulations when the quantum yield of the semiconducting polymer and the quantum dots is assumed to be 0.95, i.e. the same as that of rhodamine B. The optical efficiency for the quantum dot LSC under these hypothetical conditions is still much lower than the optical efficiency for rhodamine B, whereas the result for the Red F LSC is 50% higher than that of rhodamine B. These results once again show that the large absorption/emission band overlap of the quantum dots' spectra is a serious impediment toward the implementation of this material in LSCs. On the other hand, the results for Red F show that, indeed, the optical efficiency of LSCs greatly benefits from the small absorption/emission overlap of semiconducting polymers.

The power efficiency of the LSC/detector system will depend on the optical efficiency of the LSC as well as on the wavelength-dependent efficiency of the detector. Matching the emission of the LSC to a detector that is optimized in the region of LSC emission will allow a high power efficiency. The theoretical monochromatic peak efficiency of Si solar cells is about 48% at around 1000 nm. The monochromatic peak efficiency of GaAs is about 54% at around 850 nm. If dyes can be found such that their emission overlaps with the peak efficiency of GaAs or Si, then high power efficiencies can be obtained. For instance, if the emission of Red F lies around 850 nm, then coupling a Red F LSC to a GaAs solar cell could yield a power efficiency of approximately $23\% \times 54\% = 12\%$. The performance of Red F suggests that IR-emitting polyfluorenes may be optimal materials for LSCs. Interest is already manifest in the light-emitting diode[27] and photovoltaic[28] fields of research for synthesizing materials that absorb and emit in the IR region of the spectrum. The viability of GaAs or other band gap detectors for use as LSC detectors, however, will be determined by both the cost (higher than that of Si) and the possiblity of fabricating strips of GaAs or assembling GaAs cells along the edges of LSCs in modular fashion. Finally, to further increase the power efficiency of LSCs, antireflective coatings for enhancing absorption and promoting transmission into the detector can be more easily found because of the narrow range of the absorption and emission spectra of the dyes.

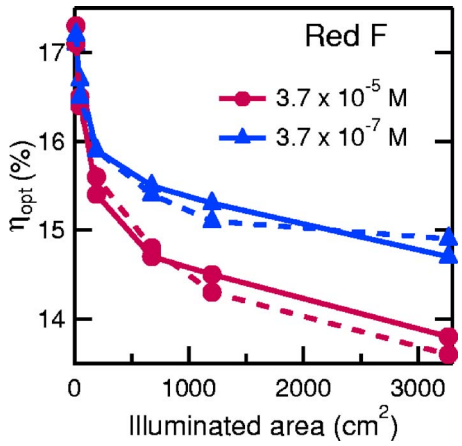

FIG. 9. (Color online) Dependence of the simulated optical efficiency of the LSCs on the illuminated area for rectangular (solid lines) and square (dotted lines) geometries of Red F LSCs at peak absorption concentration ($3.69 \times 10^{-5} M$) and peak emission concentration ($3.69 \times 10^{-7} M$).

In a practical setting, the size and shape as well as how many edges of the LSCs are coupled to detectors will depend on the cost relative to the extracted efficiency. Figures 9 and 10 present a study performed through simulations of the dependence of the optical efficiency on the size and shape of the LSC structure. Rectangular and square LSCs were simulated for illuminated (top) areas ranging between 14 cm^2 (the size of the experimental samples) and 3000 cm^2. In the case of rectangular LSCs, the area was increased while keeping the ratio of 1:3 width:length of the experimental samples. For both rectangular and square geometries, the thickness of the LSCs was kept at the thickness of the experimental samples (0.2 cm). Figure 9 shows the dependence of the optical efficiency on the top area for semiconducting polymer Red F LSCs for concentrations of peak absorption ($3.7 \times 10^{-5} M$) and of peak emission ($3.7 \times 10^{-7} M$) for the rectangular and square geometries. The similar behavior of the curves for both geometries at these extreme concentrations

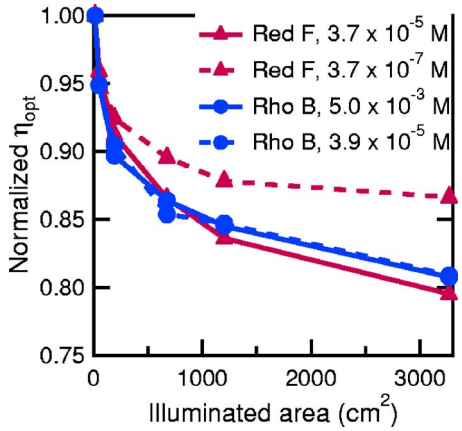

FIG. 10. (Color online) Normalized optical efficiency dependence on area for square LSCs of Rhodamine B and Red F for respective peak absorption (solid lines) and emission concentrations (dotted lines).

[This article is copyrighted as indicated in the article. Reuse of AIP content is subject to the terms at: http://scitation.aip.org/termsconditions. Downloaded to] IP: 128.114.130.190 On: Fri, 30 Jan 2015 22:00:09

suggests that the dependence of the optical efficiency on the shape of the LSCs is of minor importance. This result was verified through Monte Carlo simulations by Loh and Scalapino[12] and experimentally noted by Filloux *et al.*[29] Note that the amount of solar flux absorbed at each area value is the same for the rectangular and square geometries. How many edges of the LSC are coupled to solar cells will depend on an efficiency/cost analysis. Therefore, for full-perimeter coverage, the data suggest that squares will be the preferred geometry, since this will involve less detector surface area while keeping the amount of dye and solvent fixed, thus reducing the overall cost of the system.

Figure 10 shows the normalized simulated optical efficiency versus area for square LSCs of Red F and rhodamine B at corresponding concentrations of peak absorption and peak emission. Rhodamine B shows similar dependence of the optical efficiency on the area for the extreme concentrations given. Red F, however, shows a noticeable difference in the behavior of the efficiencies as the area increases between the high and low concentration samples. Using a sufficiently dilute dye concentration in the LSC will make the falloff of the optical efficiency with area less dramatic. This shows that sufficiently dilute solutions of Red F have small enough absorption/emission band overlap to maintain 87% of the optical efficiency of a small 14 cm^2 device. In contrast, rhodamine B shows that even at low concentrations the absorption/emission band overlap is significant to the extent that the falloff of efficiency with area cannot be avoided.

CONCLUSIONS

The motivation for this research lies in building an inexpensive solar concentrator, the LSC, by making use of semiconducting polymers and quantum dots. Previous research, centered around the use of small molecule laser dyes, was hindered by the lack of materials with small absorption/emission band overlap and longer lifetimes. We have tested semiconducting polymers and quantum dots in LSCs, since these materials may present these desirable qualities. At this stage, commercially available quantum dots do not present high enough quantum yields and small enough absorption/emission band overlaps to serve as viable LSC dyes. Materials such as Red F demonstrate that semiconducting polymers with high quantum yield are good candidates for LSCs. The development of infrared-emitting polymers for use in organic light-emitting diodes may soon provide several good LSC dyes allowing 30% LSC optical efficiencies as needed for commercial applications.

ACKNOWLEDGMENTS

One of the authors (V.S.) acknowledges Grant for Assistance in Areas of National Need (GAANN). The authors acknowledge Energy Innovations Small Grant (EISG) Program for support.

[1] A. F. Mansour, M. G. El-Shaarawy, S. M. El-Bashir, M. K. El-Mansy, and M. Hammam, Polym. Test. **21**, 277 (2002).
[2] A. F. Mansour, H. M. A. Killa, S. Abd El-Wanees, and M. Y. El-Sayed, Polym. Test. **24**, 519 (2005).
[3] W. A. Shurcliff and R. C. Jones, J. Opt. Soc. Am. **39**, 912 (1949).
[4] W. H. Weber and J. Lambe, Appl. Opt. **15**, 2299 (1976).
[5] A. Goetzberger and W. Greubel, Appl. Phys. **14**, 123 (1977).
[6] V. Wittwer, K. Heidler, A. Zastrow, and A. Goetzberger, J. Lumin. **24/25**, 873 (1981).
[7] J. S. Batchelder, A. H. Zewail, and T. Cole, Appl. Opt. **18**, 3090 (1979).
[8] M. Grande, G. Moss, S. Milward, and M. Saich, J. Phys. D **16**, 2525 (1983).
[9] R. Reisfeld, M. Eyal, V. Chernyak, and R. Zusman, Sol. Energy Mater. **17**, 439 (1988).
[10] K. Heidler, Appl. Opt. **20**, 773 (1981).
[11] J. M. Drake, M. L. Lesiecki, J. Sansregret, and W. R. L. Thomas, Appl. Opt. **21**, 2945 (1982).
[12] E. Loh and D. J. Scalapino, Appl. Opt. **25**, 1901 (1986).
[13] R. W. Olson, R. F. Loring, and M. D. Fayer, Appl. Opt. **20**, 2934 (1981).
[14] J. Roncali and F. Garnier, Appl. Opt. **23**, 2809 (1984).
[15] J. S. Batchelder, A. H. Zewail, and T. Cole, Appl. Opt. **20**, 3733 (1981).
[16] A. M. Taleb, B. T. Chiad, and Z. S. Sadik, Renewable Energy **30**, 393 (2005).
[17] A. J. Chatten, K. W. J. Barnham, B. F. Buxton, N. J. Ekins-Daukes, and M. A. Malik, Sol. Energy Mater. Sol. Cells **75**, 363 (2003).
[18] M. Kreyenschmidt *et al.*, Macromolecules **31**, 1099 (1998).
[19] B. O. Dabbousi, J. Rodriguez Viejo, F. V. Mikulec, J. R. Heine, H. Mattoussi, R. Ober, K. F. Jensen, and M. G. Bawendi, J. Phys. Chem. B **101**, 9463 (1997).
[20] K. Barnham, J. L. Marques, J. Hassard, and P. O'Brien, Appl. Phys. Lett. **76**, 1197 (2000).
[21] D. Avnir, D. Levy, and R. Reisfeld, J. Phys. Chem. **88**, 5956 (1984).
[22] R. Reisfeld, D. Shamrakov, and C. Jorgensen, Sol. Energy Mater. Sol. Cells **33**, 417 (1994).
[23] A. F. Mansour, Polym. Test. **23**, 247 (2004).
[24] T. Karstens and K. Kobs, J. Phys. Chem. **84**, 1871 (1980).
[25] C. V. Bindhu and S. S. Harilal, Anal. Sci. **17**, 141 (2001).
[26] O. I. Mićić, C. J. Curtis, K. M. Jones, J. R. Sprague, and A. J. Nozik, J. Phys. Chem. **98**, 4966 (1994).
[27] F. Zhang, E. Perzon, X. Wang, W. Mammo, M. R. Andersson, and O. Inganas, Adv. Funct. Mater. **15**, 745 (2005).
[28] M. Chen, E. Perzon, M. R. Andersson, S. Marcinkevicius, S. K. M. Jönsson, M. Fahlman, and M. Berggren, Appl. Phys. Lett. **84**, 3570 (2004).
[29] A. Filloux, J. Mugnier, J. Bourson, and B. Valuer, Rev. Phys. Appl. **18**, 273 (1983).

[This article is copyrighted as indicated in the article. Reuse of AIP content is subject to the terms at: http://scitation.aip.org/termsconditions. Downloaded to] IP: 128.114.130.190 On: Fri, 30 Jan 2015 22:00:09